A Novel Method for Indirect Estimation of Tire Pressure

Selim Solmaz
Gediz University, Department of Mechanical Engineering
Seyrek, Menemen, Izmir, 35665, TURKEY
E-mail: selim.solmaz@gediz.edu.tr

***Abstract*—In this paper a novel algorithm for indirectly estimating predetermined levels of tire deflation of an automotive vehicle is described. The estimation method is based on measuring varying levels of lateral dynamics behavior due to certain types of tire failures that may include excessive deflation or significant thread loss. Given the fact that both failures will notably affect the lateral vehicle behavior, quantifying these levels of alteration in the lateral dynamical response forms the basis of the estimation method. In achieving this, multiple models and switching method is utilized based on linearized lateral dynamics models of the vehicle that are parametrized to account for the uncertainty in tire pressure levels. The results are demonstrated using representative numerical simulations.**

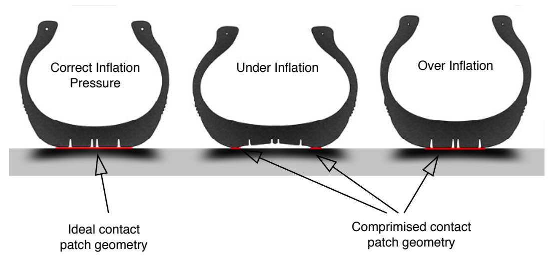

Fig. 1. Effect of inflation pressure on the tire contact patch geometry

I. Introduction

From the perspective of road safety, tires are the most important components of automotive vehicles. Tires are responsible for providing sufficient longitudinal and lateral traction (i.e., road holding) as well as directional stability. Two important factors in guaranteeing good tire functioning are related to inflation pressure and thread depth. A compromise in either factor will lead to increased braking distances, less directional stability, and increased fuel consumption levels due to reduced tire traction. It is evident that vehicles with such tire faults have comparatively poorer handling and reduced road holding, which will consequently increase their chances to be involved in road accidents.

The effect of reduced pressure and thread loss in a single or multiple tires of an automotive vehicle are very similar and are hard to distinguish by observing the changes in the lateral dynamics alone. Given the fact that the change of tire thread depth is relatively slower than the changes in tire pressure levels, the variation of tire thread depth is ignored in this study. In fact, what is of interest here is the detection of sudden pressure drops in the tires due to possible punctures well ahead of time, which may pose extreme risks while driving especially at high speeds.

It is well known that a sufficient inflation pressure level is required to support the wheel loads as well as for guaranteeing good tire functioning. A compromised tire pressure often causes a reduced tire contact patch geometry as seen in Figure 1, which results in loss of traction endangering vehicle safety. Particularly, during high speed driving, emergency braking, and rapid cornering maneuvers the tires reach their adhesion limits quickly and the corresponding tires with compromised contact patch geometry may easily loose grip affecting the vehicle's directional stability. The importance of tire safety in general, and tire pressure in specific, is also evidenced by some recent legislations in certain countries. For example the Tread Act in the USA makes it mandatory for all light duty vehicles (i.e., vehicles with a gross weight less than 4.5 tones) manufactured after September 2007 to have "Tire Pressure Monitoring System" (TPMS) [1]. Specifically the TPMS system is required to notify the driver if one or more tires are deflated by at least 25% of the manufacturer's recommended pressure levels. In Europe the "UNECE Vehicle Regulations (Regulation No. 64)" is expected to set similar but tighter standards than the USA regulations, and is planned to be in effect starting in 2012 [2]. Also, similar legislations for Korea and Japan are expected to be in place approximately 1 year after the rollout of the EU TPMS regulations [3].

Based on the observations mentioned earlier, and strongly backed up by the recent and upcoming legislative regulations, the importance of tire pressure monitoring is evident for the overall vehicle and road safety. Motivated by this, techniques for realtime monitoring of tire inflation pressures are required.

The two prominent approaches for tire pressure monitoring in the literature are the "direct" measurement and the "indirect" estimation methods. Direct TPMS technologies commonly involve a sensor system within the tire valve-stem that directly measures variations in the tire pressure levels and the temperature. On the other hand, the indirect TMPS systems are designed to estimate tire pressure utilizing other available sensors that are not necessarily embedded in the vehicle tire. Specifically, all current indirect tire deflation warning systems utilize "Anti-lock Braking System" (ABS) sensors [4] that correlate increase of wheel rotational speed with reduced pressure levels in a given tire. Some more advanced

978-1-4673-5769-2/13/$31.00 ©2013 IEEE

indirect TPMS systems also utilize vertical accelerometers for detecting vibration response of the tire to aid in the indirect inferences.

Possible shortcomings of direct TPMS systems are related to the fact that dedicated sensor equipment are required in each wheel along with a wireless communication system that transmit the measured signals to a centralized receiver connected to a dedicated "Electronic Control Unit" (ECU). That is, various components are required for such direct TPMS systems and the in-tire sensors need regular maintenance (since the sensing elements operate on limited battery power) which result in high costs. It should be appreciated that this is a limiting factor for the market penetration of such systems. Indirect TPMS systems on the other hand can potentially be implemented at no additional cost by utilizing existing sensors and ECUs. However, the state of the art indirect TPMS systems typically very slow and they need to collect lots of data before an estimation can be made. Moreover they work best when the vehicle is driven straight and at constant speed and require regular calibrations, both of which are limiting factors for obtaining reliable estimations well before a fault develops.

In the current paper the aim is to obtain an alternative indirect estimation technique for tire pressure. It is well known that the lateral vehicle response will depend on available traction in each wheel and any reduction in the traction will lead to a change in the lateral response. Given certain set of sensors this observation can be utilized to correlate reduced tire pressure levels with a set of nonlinear cornering stiffnesses of an automotive vehicle. As with existing indirect TPMS systems, the described method can be implemented as a software algorithm that can be embedded in available vehicle ECUs to detect over/under inflated tires and sudden pressure drops. The sensory requirements for the algorithm coincide with "Electronic stability Control" (ESC) system [5] sensors. ESC systems are active control systems that ensure yaw and lateral dynamics stability by using differential braking a means for control. ESC and systems with similar functionality have already a good market penetration and are available on many new modern road vehicles. They are even required in some countries as a standard fitment (e.g., from September 1st, 2011 all light duty vehicles need an ESC as a standard equipment in the USA [6]). Consequently the required sensor set for the algorithm will be assumed to be available as the same sensors are used in ESC systems. The specific sensor information required include lateral acceleration, yaw rate, steering angle, and vehicle speed. These measurements are used to drive a number of vehicle models that are parametrized to represent hypothetical vehicle lateral dynamics behavior corresponding to each different pressure level in each tire. The resulting model outputs of lateral acceleration and yaw rate are compared to that of the measured signals through a non-linear cost function to categorize the type of the tire failure in the vehicle, when and if it exists. A major benefit of this approach is that it can provide the tire pressure monitoring during cornering of the vehicle in real time, where alternative indirect tire pressure estimation systems are ineffective. The

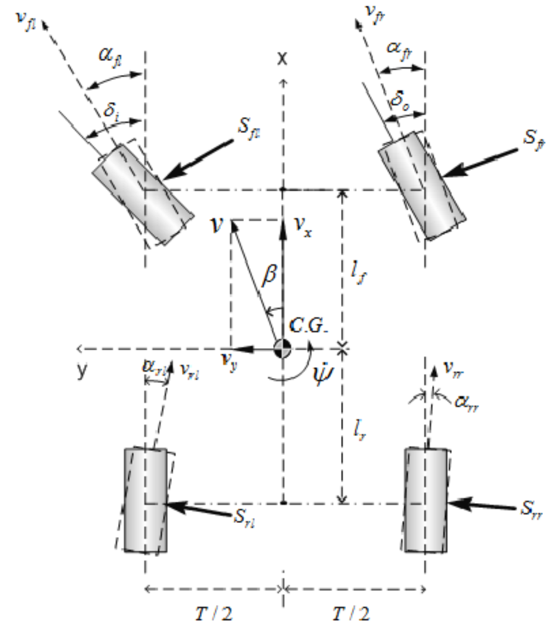

Fig. 2. Two-track vehicle model

functioning of the developed method is demonstrated with numerical simulations.

II. Vehicle and tire models

A well known vehicle dynamics model known as the 2-track vehicle model is utilized in this paper. Various abstractions of this model are derived in [7] and the reader is referred this book for the details. In this paper no roll degree of freedom is assumed and also that longitudinal speed is constant in conjunction with this model. Figure 2 shows the resulting 2-track model structure of the lateral dynamics of an automotive vehicle, which is utilized for tire condition estimation method that shall be described in Section III below.

In this model it is assumed that the vertical loads on the tires and the sideslip angles affect the lateral tire forces. Denoting the lateral tire forces as $S_{vl}, S_{vr}, S_{hl}, S_{hr}$ for front-left, front-right, rear-left and rear-right tires respectively and with reference to Figure 2, the corresponding 2-track lateral dynamics model is described as follows

$$\begin{aligned} \dot{\beta} &= \tfrac{1}{mv_x}\left[S_{vl} + S_{vr} + S_{hl} + S_{hr}\right] - \dot{\psi} \\ \ddot{\psi} &= \tfrac{1}{J_{zz}}\left[(S_{vl} + S_{vr})l_v - (S_{hl} + S_{hr})l_h\right] \end{aligned} \qquad (1)$$

It should be emphasized again that this model assumes non-linear tire models, constant vehicle speed (v_x) and no roll dynamics effects.

Since this nonlinear model has 4 tires one needs to consider the fact that the steering tires that are closer to the curb or the turning side (i.e., the inner-side) will turn with a larger angle than the outer-side wheels. In this paper this effect is modeled as a function of the steering column angle δ. The resulting asymmetric steering angles for the inner and

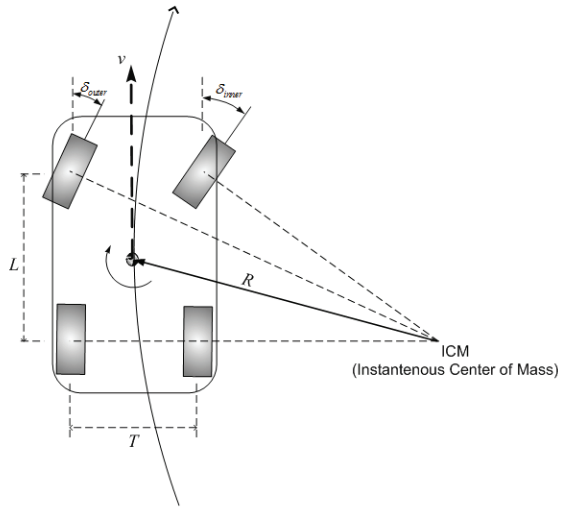

Fig. 3. Inner and outer steering angles defined with respect to the turning direction.

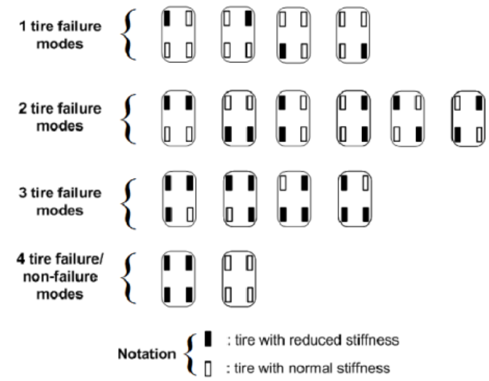

Fig. 4. Tire failure modes

outer front wheels, denoted as δ_{inner} and δ_{outer}, are defined respectively as below

$$\begin{array}{rcl} \delta_{inner} & = & \delta + \delta^2 \frac{T}{2L} \\ \delta_{outer} & = & \delta - \delta^2 \frac{T}{2L} \end{array} \tag{2}$$

The above expressions are based on a simplified model for the rotation of the front wheels about the vertical axis depicted in Figure 3. It is possible to calculate the asymmetric steering angles using alternative approaches, including use of more complicated steering geometries, or utilizing lookup tables based on real measurements for a given vehicle. The tire forces S_{ij} are nonlinear functions of the corresponding vertical tire forces F_{Zij} (wheel loads) and the tire sideslip angles α_{ij} as described below

$$\left.\begin{array}{rcl} S_{vl} & = & \left(k_{1vl} - \frac{F_{Zvl}}{k_{2vl}}\right) F_{Zvl} \arctan\left(k_{3vl}\alpha_{vl}\right) \\ S_{vr} & = & \left(k_{1vr} - \frac{F_{Zvr}}{k_{2vr}}\right) F_{Zvr} \arctan\left(k_{3vr}\alpha_{vr}\right) \\ S_{hl} & = & \left(k_{1hl} - \frac{F_{Zhl}}{k_{2hl}}\right) F_{Zhl} \arctan\left(k_{3hl}\alpha_{hl}\right) \\ S_{hr} & = & \left(k_{1hr} - \frac{F_{Zhr}}{k_{2hr}}\right) F_{Zhr} \arctan\left(k_{3hr}\alpha_{hr}\right) \end{array}\right\} \tag{3}$$

where $k_{1ij},\ k_{2ij},\ k_{3ij}$ for $i = \{v, h\}$ and $j = \{l, r\}$ are the nonlinear tire parameters. It is noted here that instead of the lateral tire model suggested in equation (3) above, one can use other alternative nonlinear tire models such as the magic formula [8] (i.e., Pacejka tire model). However for demonstration purposes only the equation (3) shall be adopted as the tire model in the sequel.

The estimation structure for the fault detection involves a set of parametrized 2-track vehicle models that take into account the tire failure modes in a multiple model configuration as shown in Figure 4. The states (i.e., the outputs) of these models are compared with the measured signals from the ESC sensor set to obtain a vector representing the identification error. Consequently the model minimizing a nonlinear cost function of the identification errors is selected. Finally, the corresponding parameterization of the selected vehicle model indicates the specific tire failure mode.

III. Multiple model estimation method

Motivated by the fact that varying lateral traction can be modeled in the lateral vehicle model by changing the tire cornering stiffness parameters, an aim of the estimation method described here is to provide an arrangement for dynamically determining the individual tire cornering stiffness values $C_{vl}, C_{vr}, C_{hl}, C_{hr}$ for each of the four tires, taking into account time variations in the vertical loads F_{Zvl}, F_{Zvr}, F_{Zhl}, F_{Zhr} acting on each tire. The side forces acting on the tires are denoted by S_{ij}, where the first index $i = \{v, h\}$ denotes "front" and "rear", and second index $j = \{l, r\}$ indicates "left" and "right", respectively (e.g., S_{vl} denotes the side force of the front left tire). Further defining α_{ij} as the side slip angle corresponding to each tire, the lateral tire force S_{ij} can then be expressed as

$$S_{ij} = C_{ij}(F_{Zij})\alpha_{ij}, \ \text{ for } \ i = \{v, h\},\ j = \{l, r\} \tag{4}$$

where $C_{ij}(F_{Zij})$ denote the dependence of time varying tire stiffnesses on the corresponding vertical forces.

In the 2-rack vehicle model utilized, the tire cornering stiffness parameters $C_{ij}(F_{Zij})$ are assumed to be unknown but their nominal values corresponding to manufacturer-recommended inflation pressures are known under changing vertical loads. Then the rationale for the estimator design given here can be explained based on the observation that when and if any of the time-varying tire cornering stiffness values (and, effectively, the corresponding lateral tire forces) are found to be smaller from the nominal levels by a certain threshold amount, then the corresponding tires must either have a non-optimal pressure (i.e., under/over inflation) resulting in a persistent loss of lateral grip. Note that the variation of the tire cornering stiffness with respect to loss of inflation pressure will vary between different tire types, but these can be measured off-line by tire manufacturers through field tests and test-rig evaluations.

Details of the operational steps of the specific indirect tire pressure estimation method based on lateral dynamics

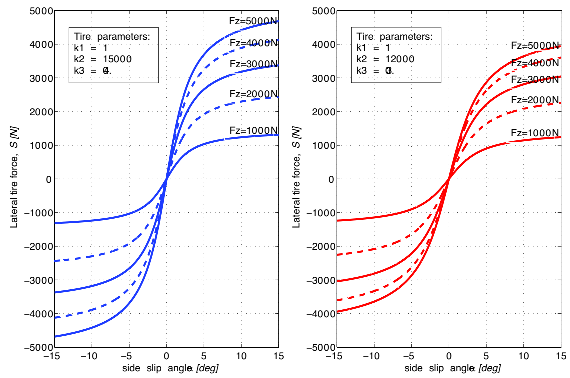

Fig. 5. Variation of lateral tire force with changing vertical force and sideslip angle for two sets of tire parameters.

measurements for calculating the lateral tire forces and the corresponding cornering stiffness parameters $C_{vl}(F_{Zvl})$, $C_{vr}(F_{Zvr})$, $C_{hl}(F_{Zhl})$, and $C_{hr}(F_{Zhr})$ the estimation method shall now be described.

Step-1: As the first step, 16 models are constructed a-priori, whose state variables are β_i and $\dot{\psi}_i$, and where $i = 1, 2, \ldots, 16$. These models are of the form (3) are are initialized such that each model corresponds to a fixed and predetermined level of cornering stiffness reduction in any combinations of the tires. In this case one needs 16 models (including the nominal model with no tire failures) which correspond to all different combinations of tire failures (in the predetermined levels) in each of the tires; this is also illustrated in Figure 4. In order to model the reduction of nonlinear cornering stiffnesses, the parameters k_{1ij}, k_{2ij}, k_{3ij} for $i = \{v, h\}$ and $j = \{l, r\}$ are selected accordingly in these 16 models.

In Figure 5 two examples of nonlinear lateral tire force variations are demonstrated as a function of changing vertical loads and changing sideslip angles, as described in equation (3). These plots exemplify a properly inflated nominal tire force variation on the left hand side, and a pressure compromised one on the right hand side.

The postulated multiple estimation model structure can eventually be expressed as follows

$$\begin{array}{rcl}\dot{\beta}_i & = & \frac{1}{mv_x}\left[S_{vl,i} + S_{vr,i} + S_{hl,i} + S_{hr,i}\right] - \dot{\psi} \\ \ddot{\psi}_i & = & \frac{1}{J_{zz}}\left[(S_{vl,i} + S_{vr,i})l_v - (S_{hl,i} + S_{hr,i})l_h\right]\end{array} \tag{5}$$

where

$$\left.\begin{array}{rcl}S_{vl,i} & = & \left(k_{1vl,i} - \frac{F_{Zvl}}{k_{2vl,i}}\right) F_{Zvl} \arctan\left(k_{3vl,i}\alpha_{vl}\right) \\ S_{vr,i} & = & \left(k_{1vr,i} - \frac{F_{Zvr}}{k_{2vr,i}}\right) F_{Zvr} \arctan\left(k_{3vr,i}\alpha_{vr}\right) \\ S_{hl,i} & = & \left(k_{1hl,i} - \frac{F_{Zhl}}{k_{2hl,i}}\right) F_{Zhl} \arctan\left(k_{3hl,i}\alpha_{hl}\right) \\ S_{hr,i} & = & \left(k_{1hr,i} - \frac{F_{Zhr}}{k_{2hr,i}}\right) F_{Zhr} \arctan\left(k_{3hr,i}\alpha_{hr}\right)\end{array}\right\} \tag{6}$$

for each $i = \{1, 2, \ldots, 16\}$. Furthermore, the method assumes zero initial conditions for each identification model, that is $\beta_i(0) = 0$ and $\dot{\psi}_i(0) = 0$.

Step-2: In the step-2, the steering column angle (δ), the vehicle velocity (v_x), the lateral acceleration (a_y), and the yaw rate $(\dot{\psi})$ are measured using the available vehicle sensors.

Step-3: In Step 3, given the measurement of lateral acceleration (ay) and provided suitable estimates of the longitudinal position of CG (l_v), the CG height (h), and the vehicle mass (m), the individual vertical tire forces corresponding to each tire are computed according to the following relations

$$\left.\begin{array}{rcl}F_{Zvl} & = & \frac{ml_h}{2L}g - \frac{ml_h h}{LT}a_y \\ F_{Zvr} & = & \frac{ml_h}{2L}g + \frac{ml_h h}{LT}a_y \\ F_{Zhl} & = & \frac{ml_v}{2L}g - \frac{ml_v h}{LT}a_y \\ F_{Zhr} & = & \frac{ml_v}{2L}g + \frac{ml_v h}{LT}a_y\end{array}\right\} \tag{7}$$

which are derived assuming a constant longitudinal vehicle speed to be consistent with the assumptions of vehicle model. Note in the above equations that the estimation of CG position (i.e, l_v and h) is required to calculate vertical force approximations for each tire. CG estimation is outside the scope of the current paper; see [9] for an example of a real time CG position estimation algorithm.

Step-4: In step 4 of the method, inner & outer steering angles δ_{inner}, δ_{outer} are computed from (2).

Step-5: In step 5, the calculated steer angles δ_{inner}, and δ_{outer} along with the measured vehicle velocity (v_x), and the yaw rate $(\dot{\psi})$ are used to compute the tire sideslip angles α_{ij} for $i = \{v, h\}$ and $j = \{l, r\}$ at each wheel depending on the turning direction as follows:

if turning left (i.e., $\delta > 0$) :

$$\left\{\begin{array}{rcl}\alpha_{vl} & = & \delta_{inner} - \arctan\left(\frac{v_x\beta + \dot{\psi}l_v}{v_x - 0.5\dot{\psi}T}\right) \\ \alpha_{vr} & = & \delta_{outer} - \arctan\left(\frac{v_x\beta + \dot{\psi}l_v}{v_x + 0.5\dot{\psi}T}\right) \\ \alpha_{hl} & = & -\arctan\left(\frac{v_x\beta - \dot{\psi}l_h}{v_x - 0.5\dot{\psi}T}\right) \\ \alpha_{hr} & = & -\arctan\left(\frac{v_x\beta - \dot{\psi}l_h}{v_x + 0.5\dot{\psi}T}\right)\end{array}\right. \tag{8}$$

if turning right (i.e., $\delta < 0$) :

$$\left\{\begin{array}{rcl}\alpha_{vl} & = & \delta_{outer} - \arctan\left(\frac{v_x\beta + \dot{\psi}l_v}{v_x + 0.5\dot{\psi}T}\right) \\ \alpha_{vr} & = & \delta_{inner} - \arctan\left(\frac{v_x\beta + \dot{\psi}l_v}{v_x - 0.5\dot{\psi}T}\right) \\ \alpha_{hl} & = & -\arctan\left(\frac{v_x\beta - \dot{\psi}l_h}{v_x + 0.5\dot{\psi}T}\right) \\ \alpha_{hr} & = & -\arctan\left(\frac{v_x\beta - \dot{\psi}l_h}{v_x - 0.5\dot{\psi}T}\right)\end{array}\right. \tag{9}$$

In the above relationships the estimate of the vehicle sideslip angle (β) is required. This is computed as a function of the available measurements using

$$\beta(t) = \int_0^t \left(\frac{a_y(\tau)}{v_x(\tau)} - \dot{\psi}(\tau)\right) d\tau \tag{10}$$

Alternatively, state observers can also be utilized to obtain an estimate of β for use in conjunction with tire slip calculations given in equations (8) and (9).

Step-6: In method Step 6, the measured vehicle velocity (v_x), and the calculated lateral tire forces S_{ij} are used to obtain the states $(\beta_i, \dot{\psi}_i)$ for each model using (5). Consequently, using the state pairs $(\beta_i, \dot{\psi}_i)$ one can then compute the lateral acceleration output corresponding to each model from

$$\left. \begin{array}{rcl} a_{y,i} & = & v_x(\dot{\beta}_i + \dot{\psi}_i) \\ & = & \frac{1}{m}\left[S_{vl,i} + S_{vr,i} + S_{hl,i} + S_{hr,i}\right] \end{array} \right\} \quad (11)$$

Step-7: In step 7 of the estimation method, the model identification error $e_i(t)$ corresponding to the i^{th} model is calculated using

$$e_i(t) = \left[\begin{array}{c} a_y(t) - a_{yi}(t) \\ \dot{\psi}(t) - \dot{\psi}_i(t) \end{array} \right] \quad \text{for} \quad i = \{1, \ldots, 16\} \quad (12)$$

Step-8: In step 8 of the method, the identification error $e_i(t)$ is used to compute the cumulative identification error $J_i(t)$ corresponding to the i^{th} model as described below

$$J_i(t) = \alpha||e_i(t)|| + \gamma \int_0^t e^{-\lambda(t-\tau)}||e_i(\tau)||d\tau \quad (13)$$

where α, γ, and λ are non-negative design parameters which can be appropriately chosen to weigh instantaneous and steady-state identification errors. This cost function is motivated by the quadratic cost optimization techniques and was suggested in [10]

Step-9: In final step of the method, the model with the least cumulative identification error is calculated using

$$i^\star = \arg \min_{i=1,\ldots,N} J_i(t) \quad (14)$$

that minimizes chooses the model with the least cost function, denoted $J_{i*}(t)$. Consequently, the instantaneous tire stiffness levels corresponding to each tire can be calculated from

$$\left. \begin{array}{rcl} C_{vl}(t) & = & C_{vl,i*}(F_{Zvl}) = \frac{S_{vl,i*}}{\alpha_{vl,i*}} \\ C_{vr}(t) & = & C_{vr,i*}(F_{Zvr}) = \frac{S_{vr,i*}}{\alpha_{vr,i*}} \\ C_{hl}(t) & = & C_{hl,i*}(F_{Zhl}) = \frac{S_{hl,i*}}{\alpha_{hl,i*}} \\ C_{hr}(t) & = & C_{hr,i*}(F_{Zhr}) = \frac{S_{hr,i*}}{\alpha_{hr,i*}} \end{array} \right\} \quad (15)$$

The procedure continues from step-2 as long as new sensor measurements are detected.

IV. Numerical simulations

In this section numerical simulations are given for the tire condition estimation algorithm. The simulation scenario involves a vehicle with a mass $m = 1300[kg]$, and with CG positions of $l_v = 1.2[m]$, $l_h = 1.3[m]$, and $h = 0.7[m]$. Also the yaw moment of inertia was set as $J_{zz} = 1200[kgm^2]$ and the track width was chosen as $T = 1.5[m]$. A 2-track lateral dynamics vehicle model with nonlinear tires provide the reference vehicle dynamics; that is, the simulated states of this model is fed as measurement signals into the recursive nonlinear tire condition estimator.

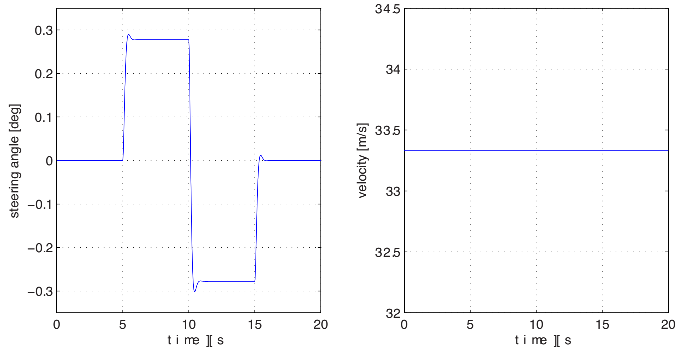

Fig. 6. Simulated input signals for the vehicle during a double lane change maneuver at constant speed.

The nominal nonlinear tire model of the form (3) and with proper inflation level was represented in the simulation with parameters $k_1 = 1$, $k_2 = 5650$, and $k_3 = 15$. The pressure compromised tires on the other hand were represented by parameters $k_1 = 1$, $k_2 = 4500$, and $k_3 = 12$. Estimation models consisted 16 switched 2-track nonlinear vehicle models of the form depicted in Figure 4 and with the above tire parameters.

The simulated maneuver involved a mild steering input representing double a lane change maneuver conducted at a constant vehicle speed of $120[km/h]$. In the simulation the failure of the front-left tire is simulated. The input signals of steering angle and velocity used for the simulation is shown in Figure 6 during a $20sec$ period.

The resulting simulation outputs are seen in Figure 7. The top 2 plots in the figure show the comparison of the simulated and estimated vehicle dynamics outputs. Note the very close estimation results in both the lateral acceleration and the yaw rate outputs. The bottom 2 plots in the Figure 7 demonstrate the switching between the estimation models during the maneuver. As can be seen form the plot, the correct estimation model (note here that 8^{th} model indicates the front-left tire failure) is selected at about 6 seconds into the simulation, which is 1 seconds into the start of the steering input causing the lateral dynamics excitation. The bottom right plot in the same figure shows how the cumulative identification errors (i.e., cost functions) grow in time for each model and the selected model cost function is indicated.

V. Conclusions and Future Directions

In this paper a novel approach for realtime estimation of tire pressure loss based on lateral dynamics measurements was presented. The specific estimation parameter used for this purpose was the tire cornering stiffness, which when found to deviate from nominal values, can be attributed to either a loss of tire pressure. The developed algorithm using a nonlinear vehicle and tire model structure was implemented in Matlab and results were demonstrated with numerical simulations. It can be conjectured that the developed method can supplement existing indirect TPMS systems as they function during

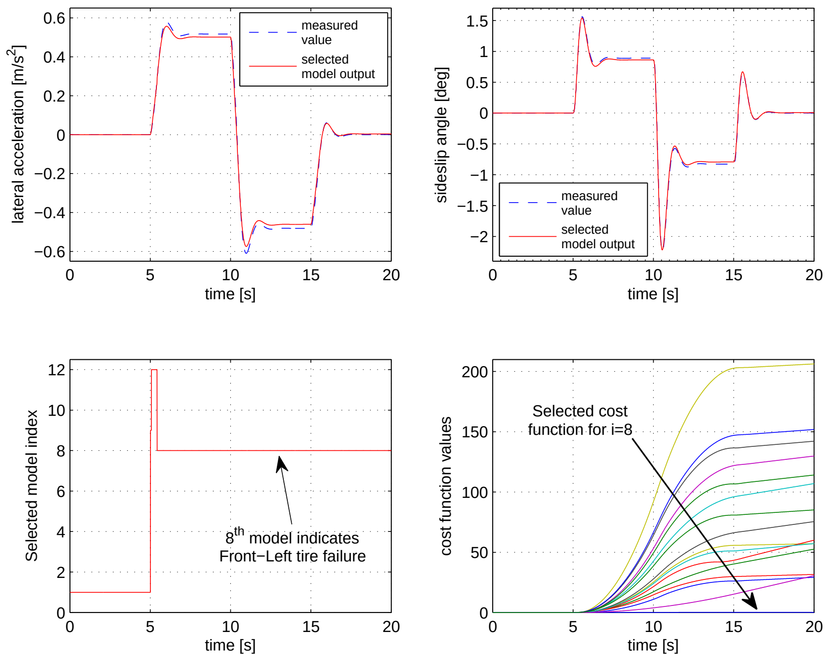

Fig. 7. Simulation results with comparison of the measured values and their switched estimates.

straight driving alone while the one described here works best during cornering.

The idea developed here can be extended in a number of ways. First and foremost, the method described in Figure **??**, can be implemented with more sets of 16 models based on equations (5) and (6) can be constructed, where each set of 16 models are initialized with different nonlinear lateral tire force characteristics as determined by the parameters k_{1ij}, k_{2ij}, k_{3ij} for $i = \{v, h\}$ and $j = \{l, r\}$. In this way, varying levels of tire failures resulting from different deflation pressures can be detected in conjunction with the suggested algorithm. A further extension could be obtained by using more complicated tire models that take into account various tire dynamical characteristics could further refine the estimations. Another research direction could be the addition of a road surface friction estimation structure into the algorithm as it is well known that high slip roads will also cause a reduced wheel traction. Therefore, there is a need to make a differentiation between traction loss due to reduced tire pressure and the loss caused by a reduced road friction. A possible approach for this is to use the brake system of the vehicle; it is known that ABS systems, commonly found in automative vehicles, provide an estimate of the road friction as part of its operation, so this can potentially feed into the tire condition estimation algorithm. Finally, the implementation and verification of the estimation algorithms on a real test vehicle is required to assess their real-time performance and robustness.

References

[1] U.S. Department of Transportation, “Federal Motor Vehicle Safety Standards, FMVSS No.138: Tire Pressure Monitoring System”, Final Regulatory Impact Analysis, March 2005.

[2] European Union UNECE Vehicle Regulations - 1958 Agreement. Addendum No.63, Regulation No.64-Rev.1 (E/ECE/324/Rev.1/Add.63/Rev.1), 9 November 2010.

[3] Wikipedia entry for “Tire-pressure monitoring system”, 20 August 2011.

[4] Gustafsson F., “Automative Safety Systems: Replacing Costly Sensors with Software Algorithms”, IEEE Signal Proc. Mag., Vol. 26, No. 4, Page(s):32-47, July 2009.

[5] Anton T. van Zanten, 2002, Evolution of Electronic Control Systems for Improving the Vehicle Dynamic Behavior. *AVEC’02 Int. Symposium on Advanced Vehicle Control*, Hiroshima, Japan.

[6] U.S. Department of Transportation, “Federal Motor Vehicle Safety Standards, FMVSS No.126: Electronic Stability Control Systems”, Final Regulatory Impact Analysis, March 2007.

[7] Kiencke U. and Nielsen L., 2000, *Automotive Control Systems for Engine, Driveline and Vehicle*, (Springer-Verlag & SAE Int., Berlin).

[8] Pacejka H.B., “Tire and Vehicle Dynamics”, 2nd Edition, SAE International, 2006.

[9] Solmaz S., Akar M., Shorten R., Kalkkuhl J., “Realtime Multiple-Model Estimation of Center of Gravity Position in Automotive Vehicles”, Vehicle System Dynamics Journal, Vol. 46, Issue. 9, Page(s):763-788, 2008.

[10] Narendra K.S. and Balakrishnan J., 1994, Improving Transient Response of Adaptive Control Systems using Multiple Models and Switching. *IEEE Transactions on Automatic Control*, Vol. 39, No. 9.

Acknowledgment

This work was partially funded by Enterprise Ireland grant PC/2008/389 and was jointly facilitated by the Hamilton Institute and Gediz University. The author wishes to thank the host institutions for their support.